Ligand Exchange Reactions between Metal(II) Chelates of Different Sulfur and Selenium Containing Ligands
IX.* Exchange Behavior of Chelates of 1,3-Dithiole-2-thione-4,5-dithiolate (dmit) and 1,1-Dichalcogenolates. X-ray Structure of $Bu_4N[Zn(dmit)(Et_2dtc)]$**

W. DIETZSCH, S. RAUER, R.-M. OLK, R. KIRMSE, K. KÖHLER

Department of Chemistry, Karl Marx University of Leipzig, DDR-7010 Leipzig (G.D.R.)

L. GOLIČ

Department of Chemistry, Edvard Kardelj University of Ljubljana, Yu-61001 Ljubljana (Yugoslavia)

and B. OLK

Central Institute of Isotopes and Radiation Research, Academy of Sciences of G.D.R., DDR-7050 Leipzig (G.D.R.)

(Received July 10, 1989)

Abstract

Nickel, copper and zinc bis-chelates of 1,3-dithiole-2-thione-4,5-dithiolate react with diethyldithio-, -thioseleno-, and diseleno-carbamates of these metals in acetone forming the mixed ligand complexes $[M(dmit)(XYCNEt_2)]^-$ (X = Y = S or Se; X = S, Y = Se) exclusively which can be isolated purely as salts of suitable cations. This synthesis can be extended to mixed ligand systems containing other geminal ligands demonstrated by $(Bu_4N)_2[Ni(dmit)(i\text{-}mnt)]$ (i-mnt = 1,1-dicyanoethene-2,2-dithiolate). EPR measurements on the copper compounds and ^1H, ^{13}C and ^{77}Se NMR measurements on the nickel and zinc systems as well show that the four-membered chelate ring gains electron density in disfavor of the five-membered chelate ring during the mixed ligand complex formation. The ligand exchange reaction between the nickel complexes can be followed by means of UV–Vis spectroscopy. All reactions obey formally a second order rate law.

The crystal and molecular structure of $Bu_4N[Zn(dmit)(Et_2dtc)]$ is reported. The compound crystallizes orthorhombic, space group $Pna2_1$ with four molecules in the unit cell; $a = 22.573(4)$, $b = 9.892(1)$, $c = 14.964(3)$ Å. Distorted tetrahedral coordination geometry is found for the ZnS_4 moiety with a dihedral angle of 89.6(2)° between the chelate planes. The Zn–S distances in the dithiolene (dmit) part of the molecule are clearly shortened in comparison to $(Bu_4N)_2[Zn(dmit)_2]$.

*For Part VIII, see ref. 8.

**Tetra-n-butylammonium(1,3-dithiole-2-thione-4,5-dithiolato)(dithiocarbamato)zincate(II).

Introduction

Depending on the chelate ring sizes ligand exchange reactions between Cu(II), Ni(II) and Zn(II) chelates containing unsaturated sulfur and/or selenium donor ligands could be classified. The most important result for synthetic purposes was that mixtures of metal chelates of geminal dichalcogeno ligands and metal chelates of vicinal dichalcogeno ligands (dithiolenes, demonstrated using maleonitriledithiolate, mnt) form the mixed ligand compounds exclusively by chelate metathesis (1) if suitable solvents are used [1–8].

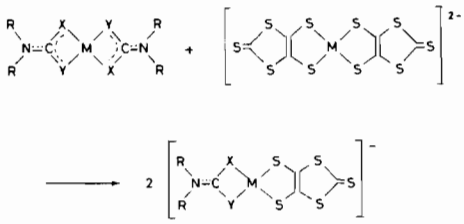

(1)

X = Y = S or Se; X = S, Y = Se

During our work on the coordination chemistry of the dithiolene ligand 1,3-dithiole-2-thione-4,5-dithiolate we found, besides different spin Hamiltonian parameters, especially in the EPR spectra of the copper complex [9] a ligand exchange behavior which does not agree completely with that of the maleonitriledithiolate chelates. Obviously, the kind of solvent used for the metathetical reactions is quite important. Changes in the absorption spectra are more drastic and allow in connection with favorable exchange reaction rates in the case of nickel complexes these reactions to be followed by UV–Vis

0020-1693/90/$3.50

spectroscopy and estimation of kinetic parameters to be made.

Several X-ray structure analyses confirmed the planar coordination geometry of such mixed ligand systems containing Cu(II) or Ni(II) central ions: $Bu_4N[Cu(mnt)(Bu_2dtc)]$ (Bu_2dtc = di-n-butyldithiocarbamate) [10], $Bu_4N[Ni(mnt)(Et_2dsc)]$ (Et_2dsc = diethyldiselenocarbamate) [3], $(Et_4N)_2[Ni(mnt)(i\text{-}mns)]$ (i-mns = 1,1-dicyanoethene-2,2-diselenolate) [5], $Bu_4N[Ni(mnt)(EtHdtp)]\cdot 0.7$acetone (EtHdtp = monoethyldithiophosphate) [4] and $Bu_4N[Ni(mnt)(Et_2tsc)]\cdot 0.5$acetone ($Et_2tsc$ = diethylthioselenocarbamate) [8]. The structure of only one nearly tetrahedral coordinated mixed ligand system has been published up to now: the dihedral angle between the mnt plane and the CS_2 plane in the dithiocarbamate in $Ph_4As[Zn(mnt)(Et_2dtc)]$ was found to be 87.6° [7]. In this paper we report the X-ray structure of another tetrahedrally coordinated mixed ligand complex, $Bu_4N[Zn(dmit)(Et_2dtc)]$, the first one containing a dmit ligand.

Experimental

Preparation of Compounds

The ligands used in this work as well as the pure parent complexes have been prepared by standard literature methods.

$Bu_4N[Cu(dmit)L]$ (L = Et_2dtc, Et_2tsc, Et_2dsc) can be prepared starting with 0.25 mmol (235 mg) $(Bu_4N)_2[Cu(dmit)_2]$, dissolved in 50 ml acetone, and 0.275 mmol bis(dichalcogenocarbamato)copper(II), dissolved also in at least 50 ml acetone. The metathetical reaction is very fast (can be checked by electron spin resonance spectroscopy [6]). Addition of isopropanol and slow reduction of the volume *in vacuo* yields brown crystals which can be recrystallized from acetone–isopropanol in the same way.

$Bu_4N[Zn(dmit)L]$ (L = Et_2dtc, Et_2dsc) can be obtained starting with the parent zinc compounds in a similar procedure to that described for copper complexes using a mixture of n-heptane and isopropanol (1:1) instead of pure isopropanol. Unfortunately, with thioselenocarbamate no solid compound could be isolated. Trying Ph_4As^+ as the cation yielded a solid product which could not completely be purified, however, the purity was sufficient for NMR spectroscopic purposes.

$Bu_4N[Ni(dmit)L]$ (L = Et_2dtc, Et_2tsc, Et_2dsc) are formed in a slow metathetical reaction in acetone. The unified starting solutions (in the same ratio as described for copper compounds) are refluxed until the color changes from dark green to dark red (at least 20 min). Crude products crystallize after addition of isopropanol and reduction of the volume *in vacuo*. The red compounds can be recrystallized from acetone–isopropanol.

TABLE 1. Physical properties of the prepared mixed ligand chelates $Bu_4N[M(dmit)L]$ and $(Bu_4N)_2[Ni(dmit)(i\text{-}mnt)]$

M	L	Melting point (°C)	Color	Λ [a]
Ni	Et_2dtc	145/50	dark red	91
	Et_2tsc	140/2	dark red	100
	Et_2dsc	140/3	dark red	89
Ni	i-mnt	127/9	dark red	195
Cu	Et_2dtc	113/6	dark brown	97
	Et_2tsc	99/103	dark brown	100
	Et_2dsc	108/12	dark brown	88
Zn	Et_2dtc	89/91	orange	94
	Et_2dsc	87/9	orange	88

[a] $Ohm^{-1}\ cm^2\ mol^{-1}$; measured in acetone, $T = 298$ K, $c = 10^{-4}$ M.

$(Bu_4N)_2[Ni(dmit)(i\text{-}mnt)]$ can be prepared starting with $(Bu_4N)_2[Ni(dmit)_2]$ and $(Bu_4N)_2[Ni(i\text{-}mnt)_2]$ in the same manner as described for the dichalcogenocarbamate compounds.

All new compounds have been verified by elemental analyses, summarized with their physical properties in Table 1.

Physical Measurements

^1H, ^{13}C and ^{77}Se NMR spectra were recorded on a Bruker AM 250 spectrometer operating at 250, 62.9 and 47.8 MHz, respectively. EPR spectra were taken at room temperature using an E-112 spectrometer (VARIAN) in the X-band. Absorption spectra for kinetic investigations were measured on a Perkin-Elmer 330 spectrometer. The molar conductivities were measured using a conductivity bridge LM 301 (VEB Hydromat Bannewitz).

Crystal Data, Intensity Data, Structure Determination and Refinement

Suitable crystals of $Bu_4N[Zn(dmit)(Et_2dtc)]$ could be grown by slow evaporation of an acetonic solution which contained a few drops of ethanol.

A rectangular plate with the approximate dimensions 0.65 × 0.67 × 0.02 mm was used for data collection on an Enraf-Nonius CAD-4 diffractometer with graphite monochromatized Mo Kα radiation. The cell parameters were determined by a least-squares treatment of 75 θ values in the range $10 \leqslant \theta \leqslant 14°$ using the Mo $K\alpha_1$ wave length with a value of 0.70926 Å. A hemisphere of data with $1 \leqslant \theta$ was measured at room temperature (293(1) K) with ω–2θ scan, scan width $(0.7 + 0.3 \text{ tg } \theta)°$, aperture $(2.4 + 0.9 \text{ tg } \theta)$ mm, scan speed 1.03–5.49 °/min and maximum scan time 60 s. Three standard reflections were monitored after every 15000 s of measuring time. A linear decay in the intensity of standard

TABLE 2. Details of the crystallographic data

Formula	$C_{24}H_{46}N_2S_7Zn$
Formula weight	652.46
Temperature (K)	293(1)
Space group	$Pna2_1$ (No: 33)
a (Å)	22.573(4)
b (Å)	9.892(1)
c (Å)	14.964(3)
V (Å^3)	3341(2)
Z	4
D_m (Mg m^{-3})	1.29(1)
D_{calc} (Mg m^{-3})	1.297
Radiation	Mo Kα (0.71069 Å)
Linear absorption coefficient (mm^{-1})	1.19
Data limits (°)	$1 \leq \theta \leq 25$
Total no. data collected	12515
Average, R_{int}	0.04
Total no. unique data	3053
No. unique data with $I > 2.5\sigma$	1173
No. contributing reflections	1534
No. variable parameters	306
R	0.032
R_w	0.038

reflections to 85.7% of the original values was observed and a correction applied. Owing to the low value of the linear absorption coefficient no absorption correction was applied. The intensity distribution suggested a acentric space group. This choice was confirmed by the successful solution and refinement of the structure. Further details concerning data collection are given in Table 2.

The zinc atom position was determined by a Patterson map. All remaining non-hydrogen atoms were located from successive Fourier maps. The hydrogen atoms, confirmed from the difference map, were placed at calculated positions with isotropic temperature factors of the attached atoms and included as fixed atom contribution in the structure factor calculations. Two blocks matrix least-squares refinement on F magnitudes with anisotropic temperature factors for all non-hydrogen atoms, using the empirical weighting function $w = W_f \times W_s$ where $W_f(|F_o| < 20.0) = |F_o|/20.0$, $W_f(|F_o| > 32.0) = 32.0/|F_o|$, $W_f(20.0 < |F_o| < 32.0) = 1.0$ and $W_s(\sin\theta < 0.30) = (\sin\theta/0.30)^{1.5}$, $W_s(\sin\theta > 0.31) = (0.31/\sin\theta)^{4.0}$, $W_s(0.30 < \sin\theta < 0.31) = 1.0$ to keep $\Sigma w(\Delta F)^2$ uniform converged to R values listed in Table 2. Atomic scattering factors for hydrogen atoms were taken from Stewart *et al.* [11], for other neutral atoms from Cromer and Mann [12] and dispersion corrections from Cromer and Liberman [13]. All calculations were performed on the DEC-10 computer at RCU-Ljubljana using XRAY76 [14] system of crystallographic programs.

Results and Discussion

As known for the maleonitriledithiolate ligand, bis-complexes of 1,3-dithiole-2-thione-4,5-dithiolate in metathetical reactions with complexes of 1,1-dichalcogeno ligands (e.g. dichalcogenocarbamates) in suitable solvents also form the mixed ligand complexes exclusively, according to eqn. (2).

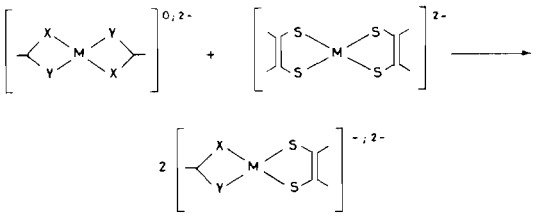

X = Y = S or Se; X = S, Y = Se

For M = Cu and Zn the exchange reactions are very fast whilst nickel complexes react quite slowly because of their higher inertness.

EPR Investigations

In contrast to exchange reactions where mnt complexes are involved the reactions of dmit compounds are not solvent-independent. The solvent governs the ratio between the starting and the mixed ligand complexes, which can be checked very easily by EPR. Figure 1(a) shows the EPR spectrum of $Bu_4N[Cu(dmit)(Et_2dsc)]$ dissolved in acetone. Only signals of this mixed ligand species are to be seen exhibiting ^{77}Se satellites in the expected relative intensity. The same compound dissolved in chloroform gives, however, EPR patterns of three species: the two parent complexes in equilibrium with the mixed ligand one (Fig. 1(b)). This holds also for combinations with dithio- and thioselenocarbamate ligands. Acetone seems to be the most favorable solvent for the preparation of pure samples of mixed ligand complex salts.

As published earlier [9] the g value of $[Cu(dmit)_2]^{2-}$ is noticeable larger (2.052) than that measured for other copper dithiolene complexes. Therefore, there should be differences also in the g values of Cu mixed ligand complexes with dmit as one ligand compared with those containing mnt. This means, that the linear dependence of the g value on the composition of the S_nSe_{4-n} (n = 0–4) coordination sphere found earlier for $[Cu(mnt)L]^-$ chelates [1] cannot be used for an unambiguous characterization of the possible $[Cu(dmit)L]^-$ mixed ligand species. This can be seen from Table 3 which summarizes the spin Hamiltonian parameters of the parent and mixed ligand complexes under study and allows a comparison to those of the corresponding $[Cu(mnt)L]^-$ chelates. The g values of the $[Cu(dmit)L]^-$ complexes are found to be also linearly

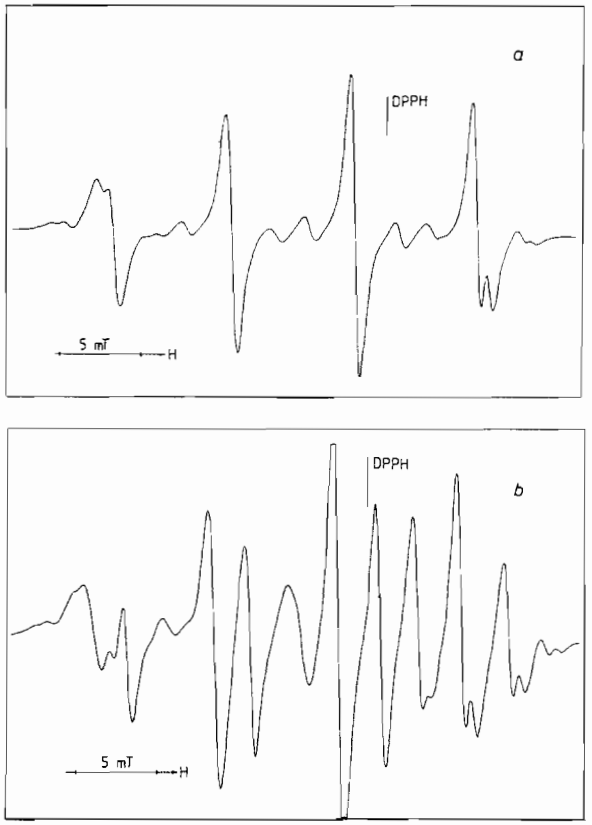

Fig. 1. EPR spectrum of $Bu_4N[Cu(dmit)(Et_2dsc)]$ dissolved in acetone (a) or chloroform (b).

TABLE 3. Comparison of spin Hamiltonian parameters[a] of parent and mixed ligand chelates (a_0 in 10^{-4} cm^{-1}) measured in acetonic (Cu dichalcogenocarbamates in $CHCl_3$) solution

Compound	g_0	a_0^{Se}	a_0^{Cu}	Reference
$Cu(Et_2dtc)_2$	2.046		75.0	15
$Cu(Et_2tsc)_2$	2.032	42.8	74.0	16
$Cu(Et_2dsc)_2$	2.020	44.5	76.0	17
$[Cu(dmit)_2]^{2-}$	2.052		70.0	9
$[Cu(dmit)(Et_2dtc)]^-$	2.048		72.5	
$[Cu(dmit)(Et_2tsc)]^-$	2.043	52.5	72.0	
$[Cu(dmit)(Et_2dsc)]^-$	2.038	54.0	72.0	
$[Cu(mnt)]^{2-}$	2.045		80.0	18
$[Cu(mnt)(Et_2dtc)]^-$ [b]	2.043		80.4	19
$[Cu(mnt)(Et_2tsc)]^-$	2.040	52.8	74.8	20
$[Cu(mnt)(Et_2dsc)]^-$	2.034	53.2	75.3	20

[a]Experimental errors: $g_0 \pm 0.002$; $a_0^{Se} \pm 0.5$; $a_0^{Cu} \pm 0.5$. [b]Measured in a $Bu_4N[Cu/Ni(mnt)(Et_2dtc)]$ single crystal.

dependent on the S/Se ratio in the coordination sphere as were those of the $[Cu(mnt)L]^-$ species. Nevertheless because of the closeness of the g parameters of the different CuS_nSe_{4-n} species, this study shows that puzzling results can be obtained if new ligands are included. Although the coordination spheres of the complexes are the same, changes in the electron density on the donor atoms can have a noticeable effect on the EPR parameters.

Generally the selenium-77 superhyperfine splitting in the spectra of the mixed ligand systems is larger than found for the parent dichalcogenocarbamates (see Table 3). Not taking into account possible symmetry changes, this means that during the chelate metathesis the four-membered chelate ring gains unpaired electron density in disfavor of the five-membered chelate ring in the starting complexes.

Kinetic Investigations

As mentioned before, the ligand exchange of the nickel complexes can be followed by UV–Vis spectroscopy. As shown in Fig. 2 there are strong differences in the spectra of the starting complexes and the mixed ligand complexes. However, in contrast to the dichalcogenocarbamate compounds used, $[Ni(dmit)_2]^{2-}$ in acetonic solution is not light stable over a long period. It is shown that dmit bis-chelates can be oxidized photochemically [21]. Therefore, it is necessary to correct kinetic measurements according to the dropping concentration of $[Ni(dmit)_2]^{2-}$. For kinetic measurements we chose the decrease of the band at 620 nm during the chelate metathesis. This absorption was also used to check the 'decomposition' of the $[Ni(dmit)_2]^{2-}$ complex when exposed to diffuse daylight. A spectrum was taken every 30 min: after 120 min 93% and after 240 min 84% of the initial concentration was found.

After unification of the two starting solutions a spectrum was recorded every 30 min. The existence of isosbestic points shows that no side reactions occurred. In Fig. 3 the changes in the spectra during chelate metathesis at room temperature between $[Ni(dmit)_2]^{2-}$ and $Ni(Et_2dtc)_2$ or $Ni(Et_2dsc)_2$ are shown. As published for other ligand exchange reactions [6], the reactions under study follow

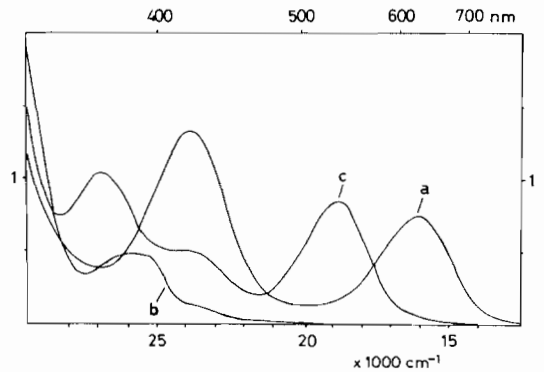

Fig. 2. UV–Vis spectra of $(Bu_4N)_2[Ni(dmit)_2]$ (a), $Ni(Et_2dtc)_2$ (b) and $Bu_4N[Ni(dmit)(Et_2dtc)]$ (c) (10^{-4} M in acetone).

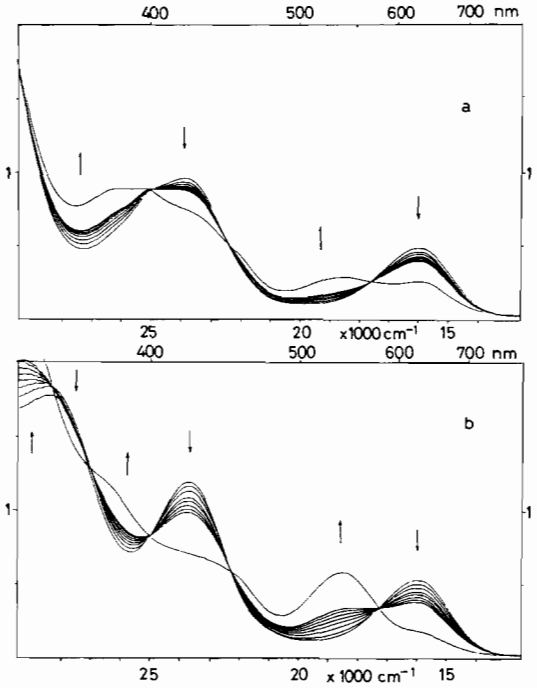

Fig. 3. Time-dependent changes in the electronic spectra of equimolar (10^{-4} M in acetone) mixtures of $(Bu_4N)_2[Ni(dmit)_2]$ and $Ni(Et_2dtc)_2$ (a) or $Ni(Et_2dsc)_2$ (b) (8 times every 30 min, last run after 24 h).

formally a second order rate law. The real mechanism of these reactions seems to be rather complicated. Obviously they obey a chain mechanism starting with a dissociative step as was shown earlier [22]. The following rate constants for the exchange reactions

$$[Ni(dmit)_2]^{2-} + NiL_2 \longrightarrow 2[Ni(dmit)L]^-$$

were estimated as

L = Et_2dtc: $k_2 = (0.43 \pm 0.02)$ l mol^{-1} s^{-1}

Et_2tsc: (0.75 ± 0.02) l mol^{-1} s^{-1}

Et_2dsc: (2.5 ± 0.3) l mol^{-1} s^{-1}

Three points are worth noting. (i) The more selenium donor atoms participate in the chelate metathesis the more the reaction rate increases. (ii) Three hundred to some thousand times higher reaction rates were measured when copper complexes were also involved (e.g. $[Cu(dmit)_2]^{2-}/Ni(Et_2dsc)_2$: $(2.5 \pm 0.3) \times 10^2$; $[Cu(mnt)_2]^{2-}/Ni(Et_2dsc)_2$: $(2.1 \pm 0.1) \times 10^2$; $Cu(Et_2dtc)_2/Cu(Et_2dsc)_2$: $(2.0 \pm 0.3) \times 10^4$ l mol^{-1} s^{-1} [6]). (iii) Independent of the ligand type these ligand exchange reactions obey the same mechanism.

NMR Measurements

To answer the question if there are strong differences in the electronic structures of the parent and the mixed ligand complexes we investigated some copper complex combinations by EPR and found a gain in spin density for the four-membered chelate rings in disfavor of the five-membered chelate rings in comparison to the parent complexes [1, 3, 23]. ^{13}C NMR measurements revealed a higher shielding for the C atoms in the four-membered chelate rings in some nickel mixed ligand complexes [23]. Therefore, we also investigated the diamagnetic dmit containing nickel and zinc complexes by ^{13}C NMR and in two cases by ^{77}Se NMR. Tables 4 and 5 summarize the results. Additionally Table 6 allows a comparison of proton chemical shifts of the ethyl hydrogens of parent and mixed ligand complexes. Generally the electron density at most of the C atoms and also at the selenium donor atoms in the four-membered chelate rings is higher in the mixed ligand compounds than in the parent complexes. The situation for the carbons in the five-membered chelate rings is reversed. This means that also in these dmit systems an electron density transfer takes place from the five-membered to the four-membered chelate ring during the mixed ligand complex formation. Unfortunately the same solvent could not be used in all cases. However, as can be seen from the few examples in Table 5, the effect is apparent in different and the same solvents. Even in the proton spectra a very small effect was found.

This electron density transfer is certainly one reason for the higher stability of the heteroligand systems in comparison to the homoligand compounds.

X-ray Structure of $Bu_4N[Zn(dmit)(Et_2dtc)]$

A stereoscopic view of the unit cell content is presented in Fig. 4, and the atom labelling scheme of the anion is shown in Fig. 5. The structure consists of discrete tetra-n-butylammonium cations and $[Zn(dmit)(Et_2dtc)]^-$ anions. Selected bond distances and angles of the anion are given in Table 7. The zinc atom displays a distorted tetrahedral coordination. The least-squares planes through Zn, S(1), S(2) and C(1) and Zn, S(3), S(4), C(6) and C(7) form a dihedral angle of 89.6(4)°. This is the 'most tetrahedral' angle reported for similar compounds up to now: in the parent complex $(Bu_4N)_2[Zn(dmit)_2]$ this angle is 82(1)° [24], in the corresponding maleonitriledithiolato compound $(Ph_4As)_2[Zn(mnt)_2]$ 83.9° [25] and in the mixed ligand compound $Ph_4As[Zn(mnt)(Et_2dtc)]$ 87.6° [7]. The situation is more complicated for the parent zinc dithiocarbamate complex because it crystallizes in dimeric $Zn_2(Et_2dtc)_4$ units [7].

Although the dihedral angle in both heteroligand systems is closer to 90° than those found in the homoligand complexes, the Zn–S distances are quite different because of two different chelate ring sizes, i.e. different bite angles also, causing in this way a

TABLE 4. ^{13}C NMR chemical shifts of parent and mixed ligand complexes (ppm/TMS)[a]

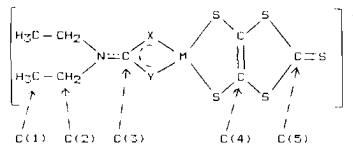

X	Y	C(1)	C(2)	(C3)	C(1)	C(2)	C(3)	C(4)	C(5)	C(4)	C(5)
		NiL_2 (in $CDCl_3$)			$[LNiL']^-$ (in DMSO-d_6)					$[NiL'_2]^{2-}$ (in DMSO-d_6)	
S	S	12.4	48.3	206.3	12.1	43.0	201.8 203.9[b]	138.3	216.7	137.9	216.5
S	Se	12.1 12.6	46.1 44.2	198.0	12.1 12.1	46.1 43.8	193.9	138.9	216.8		
Se	Se	12.6	47.9	185.8	11.9	46.4	186.4	139.4	216.9		
		ZnL_2 (in $CDCl_3$)			$[LZnL']^-$ (in DMSO-d_6)					$[ZnL'_2]^{2-}$ (in DMSO-d_6)	
S	S	12.1	49.4	201.9 202.3[c]	11.9	48.7	200.7	134.0	207.6	135.0	206.7
S	Se	11.8 12.3	52.6 48.0	195.2	11.5 12.1	52.3 47.5	193.5	134.1	207.7		
Se	Se	11.9	51.3	187.4 188.2[c]	11.6	51.2	185.8	134.3	207.7		

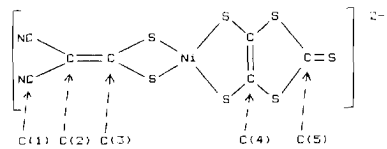

	C(1)	C(2)	C(3)	C(1)	C(2)	C(3)	C(4)	C(5)	C(4)	C(5)
	$[NiL_2]^{2-}$ (in DMSO-d_6)			$[LNiL']^{2-}$ (in DMSO-d_6)					$[NiL'_2]^{2-}$ (in DMSO-d_6)	
	116.3	70.6	214.6	115.9	68.5	211.2	138.7	216.3	137.9	216.5

[a]Ionic compounds as Bu_4N^+ salts with exception of $Ph_4As[Zn(dmit)(Et_2tsc)]$ (see 'Experimental'). [b]In $CDCl_3$. [c]In DMSO-d_6.

TABLE 5. ^1H NMR chemical shifts of ethyl protons in parent and mixed ligand complexes (ppm/TMS)[a]

Compound	$-CH_2-$	$-CH_3$
	In $CDCl_3$	
$Ni(Et_2dtc)_2$	3.60q	1.23t
$Ni(Et_2tsc)_2$	3.61q	1.23t
	3.64q	1.26t
$Ni(Et_2dsc)_2$	3.65q	1.27t
$Zn(Et_2dtc)_2$	3.87q	1.33t
$Zn(Et_2tsc)_2$	3.88q	1.34t
		1.36t
$Zn(Et_2dsc)_2$	3.90q	1.37t
	In DMSO-d_6	
$Zn(Et_2dtc)_2$	3.82q	1.22t
$Zn(Et_2tsc)_2$	3.84q	1.21t
		1.24t
$Zn(Et_2dsc)_2$	3.89q	1.28t

(continued)

TABLE 5. *(continued)*

Compound	$-CH_2-$	$-CH_3$
	In DMSO-d_6	
$[Ni(dmit)(Et_2dtc)]^-$	3.55q	1.13t
$[Ni(dmit)(Et_2tsc)]^-$	3.56q	1.14t
		1.17t
$[Ni(dmit)(Et_2dsc)]^-$	3.61q	1.18t
$[Zn(dmit)(Et_2dtc)]^-$	3.81q	1.22t
$[Zn(dmit)(Et_2tsc)]^-$	3.81q	1.22t
		1.25t
$[Zn(dmit)(Et_2dsc)]^-$	3.86q	1.26t

[a]Bu_4N^+ salts with exception of $Ph_4As[Zn(dmit)(Et_2tsc)]$ (see 'Experimental'); q = quartet, t = triplet.

substantial deviation from tetrahedral symmetry. As found for the mnt ligand in $[Zn(mnt)(Et_2dtc)]^-$ relatively to $[Zn(mnt)_2]^{2-}$ [7] the Zn–S bond lengths in the dithiolene part (dmit) of [Zn(dmit)-

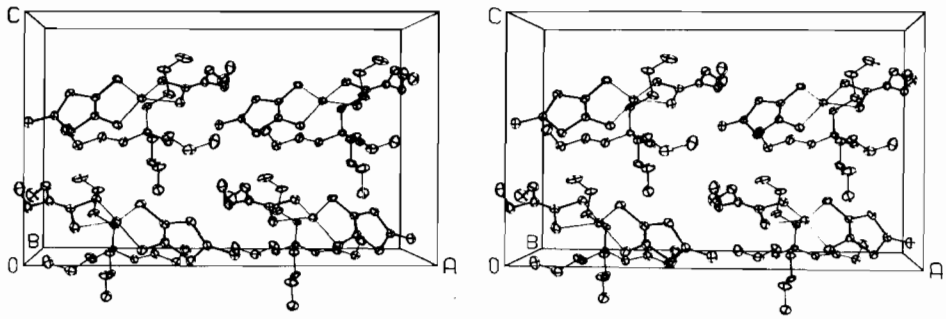

Fig. 4. Stereoview of the unit cell of $Bu_4N[Zn(dmit)(Et_2dtc)]$.

TABLE 6. ^{77}Se NMR chemical shifts of zinc parent and mixed ligand complexes in DMSO-d_6 (ppm/H_2SeO_3)

X	Y	$Zn(XYCNEt_2)_2$	$[Zn(dmit)(XYCNEt_2)]^-$ [a]
S	Se	−692.7	−713.3
Se	Se	−633.4	−638.9

[a] $Ph_4As[Zn(dmit)(Et_2tsc)]$ and $Bu_4N[Zn(dmit)(Et_2dsc)]$.

$(Et_2dtc)]^-$ are clearly shortened in comparison to $[Zn(dmit)_2]^{2-}$ (2.338(2) Å [24]) suggesting a similarity in the electronic nature of $[Zn(mnt)(Et_2dtc)]^-$ and $[Zn(dmit)(Et_2dtc)]^-$.

The twelve C–C bonds in the aliphatic chains of the tetra-n-butylammonium cations are remarkably shorter than expected for the standard $C(sp^3)$–$C(sp^3)$ distance (1.46(2) to 1.53(2) Å; average 1.50(2) Å). The four N–C–C angles (115.9(8), 116.6(8), 116.6(8), 116.3(9)°; average 116.4(3)°) deviate considerably from the tetrahedral value indicating a strong deformation of the cations by steric hindrance due to packing in the structure.

The shortest interionic contact is 3.68(1) Å between S(6) and C(24).

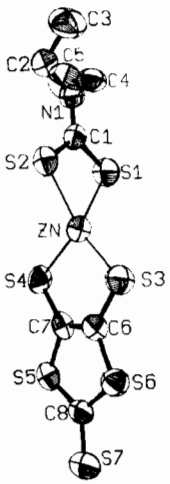

Fig. 5. Structure and atom numbering of the anion $[Zn(dmit)(Et_2dtc)]^-$.

TABLE 7. Selected bond lengths (Å) and angles (°) for the anion $[Zn(dmit)(Et_2dtc)]^-$

Zn–S1	2.373(3)	Zn–S3	2.277(3)
Zn–S2	2.399(3)	Zn–S4	2.319(3)
S1–C1	1.728(10)	S3–C6	1.765(10)
S2–C1	1.735(11)	S4–C7	1.724(10)
N1–C1	1.29(1)	S5–C7	1.748(9)
N1–C2	1.48(2)	S5–C8	1.717(11)
N1–C4	1.48(1)	S6–C6	1.735(10)
C2–C3	1.49(2)	S6–C8	1.725(11)
C4–C5	1.52(2)	S7–C8	1.645(11)
		C6–C7	1.37(1)
S1–Zn–S2	75.7(1)	S3–Zn–S4	97.5(1)
S1–C1–S2	115.6(6)	Zn–S3–C6	95.1(4)
S1–C1–N1	121.5(8)	Zn–S4–C7	94.0(3)
S2–C1–N1	123.0(7)	S3–C6–C7	125.1(8)
C2–N1–C1	122.8(9)	S4–C7–C6	128.3(7)
C2–N1–C4	115.3(9)	C6–S6–C8	98.8(5)
C4–N1–C1	121.9(9)	C7–S5–C8	100.3(5)
		S5–C8–S7	124.1(7)
		S6–C8–S7	124.8(7)
S1–Zn–S3	123.1(1)		
S1–Zn–S4	117.7(1)		
S2–Zn–S3	124.7(1)		
S2–Zn–S4	119.8(1)		

Supplementary Material

Listing of atomic coordinates and isotropic thermal parameters (Table S-I), listing of anisotropic thermal parameters of non-hydrogen atoms (Table S-II), listing of calculated coordinates of hydrogen atoms (Table S-III) and a table of observed and calculated structure factors are available on request from the authors.

Acknowledgement

The authors wish to thank Dr F. Höppner (KMU Leipzig) for his help during the kinetic measurements.

References

1 W. Dietzsch, J. Reinhold, R. Kirmse, E. Hoyer, I. N. Marov and V. K. Belyaeva, *J. Inorg. Nucl. Chem., 39* (1977) 1377.
2 W. Dietzsch, J. Lerchner, J. Reinhold, J. Stach, R. Kirmse, G. Steimecke and E. Hoyer, *J. Inorg. Nucl. Chem., 42* (1980) 509.
3 J. Stach, R. Kirmse, U. Abram, W. Dietzsch, J. H. Noordik, K. Spee and C. P. Keijzers, *Polyhedron, 3* (1984) 433.
4 R. Kirmse, W. Dietzsch, J. Stach, L. Golič, R. Böttcher, W. Brunner, M. C. M. Gribnau and C. P. Keijzers, *Mol. Phys., 57* (1986) 1139.
5 H. J. Bruins Slot, J. H. Noordik, P. T. Beurskens, C. P. Keijzers, W. Dietzsch and R. Kirmse, *J. Crystallogr. Spectrosc. Res., 14* (1984) 617.
6 J. Stach, R. Kirmse, W. Dietzsch, G. Lassmann, V. K. Belyaeva and I. N. Marov, *Inorg. Chim. Acta, 96* (1985) 55.
7 I. Leban, L. Golič, R. Kirmse, J. Stach, U. Abram, J. Sieler, W. Dietzsch, H. Vergoossen and C. P. Keijzers, *Inorg. Chim. Acta, 112* (1986) 107.
8 H. J. Bruins Slot, R. C. Haltiwanger, V. Parthasarathi, M. Kolenbrander, P. T. Beurskens, W. Dietzsch and R. Kirmse, *J. Crystallogr. Spectrosc. Res., 16* (1986) 617.
9 G. Steimecke, R. Kirmse and E. Hoyer, *Z. Chem., 15* (1975) 28.
10 A. L. Spek, *Cryst. Struct. Commun., 2* (1973) 463.
11 R. F. Stewart, E. R. Davidson and W. T. Simpson, *J. Chem. Phys., 42* (1965) 3175.
12 D. T. Cromer and J. B. Mann, *Acta Crystallogr., Sect. A, 24* (1968) 321.
13 D. T. Cromer and D. J. Liberman, *J. Chem. Phys., 53* (1970) 1891.
14 J. M. Stewart, P. A. Machin, C. W. Dickinson, H. L. Ammon, H. Heck and H. Flack, *The XRAY76 System, Tech. Rep. TR-446,* Computer Science Center, University of Maryland, College Park, MD, 1976.
15 T. Vänngard, *Nature (London), 184* (1959) 183.
16 R. Heber, R. Kirmse and E. Hoyer, *Z. Anorg. Allg. Chem., 393* (1972) 159.
17 R. Kirmse, B. Lorenz, E. Hoyer and W. Windsch, *Z. Chem., 10* (1970) 305.
18 A. H. Maki, N. Edelstein, A. Davison and R. H. Holm, *J. Am. Chem. Soc., 86* (1964) 4580.
19 J. Stach, R. Kirmse, W. Dietzsch and E. Hoyer, *Inorg. Nucl. Chem. Lett., 14* (1978) 143.
20 R. Kirmse, W. Dietzsch, R. Heber and E. Hoyer, *Z. Chem., 14* (1974) 28.
21 W. Dietzsch, R.-M. Olk and J. P. Puaux, manuscript in preparation.
22 I. N. Marov, M. N. Vargaftik, V. K. Belyaeva, E. Hoyer, R. Kirmse and W. Dietzsch, *Zh. Neorg. Khim., 25* (1980) 188.
23 W. Dietzsch, U. Abram, D. Michel, D. Scheller, B. Thomas, R. Kirmse and J. Stach, manuscript in preparation.
24 H. Wang, D. Zhu, N. Zhu and H. Fu, *Acta Phys. Chim. Sin., 1* (1985) 378.
25 J. Stach, R. Kirmse, J. Sieler, U. Abram, W. Dietzsch, R. Böttcher, L. K. Hansen, H. Vergoossen, M. C. M. Gribnau and C. P. Keijzers, *Inorg. Chem., 25* (1986) 1369.